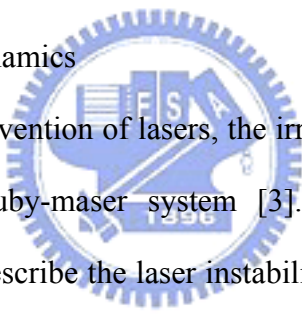# Chapter 1 Introduction

The studies on laser beams and resonators are interesting subjects in laser physics [1]. For conventional applications, one prefers to operate the laser with stable continuous-wave or periodic pulsing while sometimes one may use a chaotic laser source, for example, in chaotic communications. The problems such as spontaneous irregular pulsing, unstable mode patterns, etc., coming from intrinsic nonlinearities of the lasers are the topics of laser dynamics [2]. This field has experienced a flourishing development since late 1970s. Today laser physics still permits questions of nonlinear dynamics to be explored.

1.1 Development of laser dynamics

Almost as early as the invention of lasers, the irregular burst of short pulses was observed in a multimode ruby-maser system [3]. From then on, researchers proposed various models to describe the laser instabilities [4,5]. For example, Fleck and Kidder [6] derived a coupled-mode model from the Maxwell-Bloch equations and concluded that a moderate spatial pumping inhomogeneity could lead to coupling of two transverse modes, which gives rise to undamped spiking behavior. This field did not become popular until 1975 when Haken constructed the most famous paradigmatic model [7]. He demonstrated that the Maxwell-Bloch equations for a single mode laser are equivalent to those of the Lorenz model for fluids. This work is regarded as the cornerstone in laser dynamics. The instability of single mode laser exhibits chaotic emission under the "bad cavity" condition when the pump power is larger than nine times of the lasing threshold. In spite of difficulty, Weiss and Brock [8] experimentally observed this kind of instability by using a far infrared NH_3 laser.

For an inhomogeneously broadened laser, Casperson [9] demonstrated the

1

occurrence of transition from cw to pulsed operation. Abraham et al. [10] made further theoretical efforts for a global view of the inhomogeneous broadened laser. These instabilities with low second threshold were confirmed in a high-gain He-Xe laser [11]. Three routes to chaos including period doubling, two frequency, and intermittency scenarios [12] were observed.

The model for multimode instability was proposed by Risken and Nummedal [13], and individually by Graham and Haken [14], therefore it is known as RNGH instability. Strict experiment of RNGH instability was not realized until 1997 by using a fiber laser [15]. Another approach for modeling the multimode instability was built by Tang et al. who constructed the Tang-Statz-deMars (TSD) equations [4]. On the basis of TSD equations, K. Otsuka have studied antiphase dynamics of a $LiNdP_4O_{12}$ laser system [16].

On the other hand, it has been demonstrated that the transverse effects play important roles in laser dynamics [17]. Transverse instabilities were explored extensively by Lugiato et al. [18-23]. Under both of the uniform-field and the good-cavity limits, they expressed the Maxwell-Bloch equations through suitable empty-cavity-mode expansion because the Laguerre-Gaussian modes are a set of sensitive basis [24]. Because of the competition of transverse modes, a variety of spatiotemporal instabilities [21,22] were reported. Many efforts have been devoted to mode selection or phase control to obtain predictable behaviors [25]. Hollinger and coworkers [26] used Kirchhoff-Fresnel diffraction integral together with the rate equations to model single longitudinal multitransverse-mode lasers. They also obtained chaotic emission at specific cavities. Recently the nonlinear laser dynamics are extensively studied.

1.2   Previous research

1.2.1 Transverse mode formation

It is accepted that the eigenmodes for an open stable optical cavity form an orthogonal complete set, which means that the electric field of an arbitrary optical beam can be decomposed into the linear combination of either the Hermite-Gaussaian modes or the Laguerre-Gaussian modes [1]. In a multimode case the output intensity undergoes oscillation caused by the interference among the competing modes. In other words, the simultaneous occurrence of transverse modes, typically, is believed to imply emergency of beating effect. However, there is a stationary complex spatial structure that corresponds to nonlinear coupling of the multimodes, in which the coexisting modes "*cooperatively*" select a common frequency via the mode pulling effect and enter a regime of synchronous oscillation. Such a phenomenon was termed cooperative frequency locking (CFL) by Lugiato and collaborators [18,19]. The absence of transverse mode beating produces a stationary output pattern instead of the more familiar beating.

The extended Maxwell-Bloch equations in Ref. [21] for a ring laser are written as

$$-\frac{i}{4}\nabla_\perp{}^2 F + \frac{\partial F}{\partial \eta} + \frac{1}{v}\frac{\partial F}{\partial \tau} = i\frac{\delta\Omega}{v}F - \alpha\Lambda P,$$

$$\frac{\partial P}{\partial \tau} = -[FD + (1+i\Delta)P], \qquad\qquad (1.1)$$

$$\frac{\partial D}{\partial \tau} = -\gamma[-\frac{1}{2}(F^*P + FP^*) + D - \chi(\rho,\eta)],$$

where F is the slowly varying envelope amplitude of the electric field that is related to the Maxwell field by

$$E(r,z,t) = \frac{\hbar\sqrt{\gamma_\perp \gamma_\approx}}{2\mu}\frac{1}{2}[F(r,z,t)\exp(i(k_0 z - \omega_0 t)\times\exp(-i\delta\Omega t) + c.c.], \qquad (1.2)$$

P is the slowly varying envelope of the atomic polarization, and D is the population difference. η and ρ are the scaled longitudinal and transversal coordinates,

respectively. $\tau = \gamma_\perp t$ is the scaled time variable, $\nu = c/\Lambda\gamma_\perp$, $\gamma_\perp$ is the transverse relaxation rate, α is the unsaturated gain parameter of the field per unit length, Λ is the cavity length, $\delta\Omega$ is the frequency offset in unit of $\gamma_\perp$ between the operating laser frequency and the empty-cavity resonance ω_o, Δ is the difference between $(\omega_A - \omega_o)/\gamma_\perp$ and $\delta\Omega$, ω_A is the atomic transition frequency, $\gamma = \gamma_\approx/\gamma_\perp$, $\gamma_\approx$ is the population relaxation rate, χ is the pump profile, μ is the modulus of the atomic transition dipole moment. In the condition of the single longitudinal mode operation with uniform field limit [19] and the empty-cavity-mode expansion, i.e.,

$$\begin{bmatrix} F(\rho,\tau) \\ P(\rho,\tau) \\ D(\rho,\tau) \end{bmatrix} = \sum_{p=0}^{\infty} B_p(\rho) \begin{bmatrix} f_p(\tau) \\ p_p(\tau) \\ d_p(\tau) \end{bmatrix}, \text{ Eq. (1.1) can be transformed, according to Refs. [19]}$$

and [21], to

$$\begin{aligned}
\frac{df_p}{d\tau} &= -\kappa_p f_p - \kappa i(a_p - \Delta)f_p - 2C\kappa p_p, \\
\frac{dp_p}{d\tau} &= -\left[\sum_{q,q'} \Gamma_{pqq'} f_q d_{q'} - (1+i\Delta)p_p \right], \\
\frac{dd_p}{d\tau} &= -\gamma \left[-\frac{1}{2}\left(\sum_{q,q'} \Gamma_{pqq'} f_q^* p_{q'} + c.c. \right) + d_p - \chi_p \right].
\end{aligned} \tag{1.3}$$

Significant mode mixing and considerable distortion of the transverse intensity profiles were obtained from solving the steady-state solution of Eq. (1.3) with uniformly radial-pump profile. This stationary solution, however, has a common frequency due to strong mode-mode coupling so this phenomenon was termed as cooperative frequency locking. The analytical and numerical studies show that CFL occurs under good cavity limit ($\kappa \ll \gamma_\approx, \gamma_\perp$) for Laguerre-Gaussian basis [18] and for trigonometric basis [19] when the neighboring transverse mode spacing is small, where κ is the cavity decay rate.

1.2.2 Numerical approaches in laser dynamics

The "Recirculating Pulse" approach [1] such as the "Fox and Li" approach [27] is usually used to elucidate the physical picture of radiation, which repeatedly circulates around the cavity that contains a thin slab gain medium. The transverse mode profile can be calculated based on the central laser wavelength because the diffraction effect experienced by transverse modes will be essentially the same for those any one of the axial mode frequencies within the oscillation bandwidth. In the numerical procedure for an empty cavity, an arbitrary initial field will eventually converge to a state; that is the mode profile reproduces itself after one round trip. However, as the gain of the active medium is considered, the field may evolve automatically to a dynamical state. In our work, we use this approach to study dynamics of an end-pumped solid-state laser by using the diffraction integral together with the rate equations.

The second approach usually used in laser dynamics is the optical Maxwell-Bloch equations as described in Eq. (1.1) when the diffraction effect due to finite section of the field, the transverse gain variation, and the wave-front curvature caused by the spherical mirrors [19-21] were included. To be easily used in simulation, the electric field, atomic polarization, and the population inversion were expanded with the empty cavity modes and then the equations can be represented as the modal equations as in Eq. (1.3). The third approach is the iterative map stated below.

1.2.3 Iterative map

The iterative map is another widely used method to study the nonlinear dynamics. The study of a continuous system can be reduced to a discrete time system on a surface of section transverse to the flow. If the time period is taken as

5

the round-trip time of the laser cavity, the iterative map can be constructed. Consider a two dimensional iterative map

$$
\begin{cases}
u_{n+1} = f_1(u_n, v_n), \\
v_{n+1} = f_2(u_n, v_n),
\end{cases}
\tag{1.4}
$$

where $(u_n, v_n) = \mathbf{x}_n$ are the dynamical variables for the n-th iterations and $(f_1, f_2) = \mathbf{F}$ represents a set of difference equations. A fixed point $\mathbf{x}_0$ is therefore a stationary solution that satisfies $\mathbf{F}(\mathbf{x}_0) = \mathbf{x}_0$. If there exists the smallest positive integer p such that $\mathbf{F}^{(p)}(\mathbf{x}_0) = \mathbf{x}_0$, where $\mathbf{F}^{(p)}(\mathbf{x}_0) = \mathbf{F}(\mathbf{F}(\ldots\mathbf{F}(\mathbf{x}_0)\ldots))$, then $\mathbf{x}_0$ is said a fixed point of period-p and the orbit is a periodic orbit with period p. The stability of a fixed point can be determined by the linear stability analysis. If the system is perturbed from the fixed point and the perturbation does not be amplified, then the fixed point is stable; otherwise, it is unstable.

Applying the ABCD law in a two mirror cavity with the reference plane at one of the mirrors [28], the q-parameter $(1/q = 1/R - i\lambda/\pi w^2)$ of the Gaussian beam of the (n+1)-th round trip to the n-th one can be written as

$$
\begin{cases}
w_{n+1} = f_1(w_n, R_n) = w_n \sqrt{(A + B/R_n)^2 + \left((\lambda/\pi w_n^2)\right)^2 B^2}, \\[2mm]
R_{n+1} = f_2(w_n, R_n) = \dfrac{(A + B/R_n)^2 + \left((\lambda/\pi w_n^2)\right)^2 B^2}{(A + B/R_n)(C + D/R_n) + \left((\lambda/\pi w_n^2)\right)^2 BD},
\end{cases}
\tag{1.5}
$$

where w is the spot size and R is the radius of curvature. This map belongs to the conservative one because the resonator is lossless. The stability condition $\left|Tr(J_p)\right| <$ 2 depends only on the trace $Tr(J_p)$ with the Jocobian matrix J_p evaluated at the studied fixed point. The stability condition depends on the residue that defined as [29] $\mathrm{Re}\, s = \frac{1}{4}\left(2 - Tr(J_p)\right) = \sin^2(\theta/2)$, where θ is the phase shift per iteration of the map. For 0 < Res < 1, the system is stable that corresponds to the conventional geometric stable regime $0 < g_1 g_2 < 1$, where $g_{1,2} = (1 - d/R_{1,2})$ of the two-mirror cavity is the

so-called g-parameter of the optical cavity. For Res < 0 and Res >1, the system is unstable. By applying the Greene's residue theorem, Wei et al. [30] indicated that the special case of Res = 0, 1, 3/4, 1/2 correspond to the low order resonance that correspond to the cavity configuration with specific g_1g_2 parameter. For a simple two mirror cavity, Res = $1-(2g_1g_2 -1)^2$ = 0 (critical stable) corresponds to g_1g_2 = 0 and 1; Res = 1 (critical stable) to g_1g_2 = 1/2; Res = 3/4 to g_1g_2 = 1/4 and 3/4; and Res = 1/2 to $g_1g_2 = \dfrac{2 \pm \sqrt{2}}{4}$, respectively.

The dynamical behavior can be realized from constructing the iterative map of Eq. (1.5). Figure 1.1(a) is a period-2 evolution that shows the spot size flip-flops at two values for the case of g_1g_2 = 1/2. When a Gaussian aperture was added in the cavity, the spot size evolves to a convergent value as shown in Fig. 1.1(b). A quasi-periodic evolution of the two-dimensional map was drawn in the phase space of (1/R, w) in Fig. 1.2(a) for g_1g_2 = 0.9. The evolution of spot size shown in Fig. 1.2(b) exhibits some oscillating braches and converges to a value when a loss component was added [Fig. 1.2(c)].

The aforementioned dynamics depending on the cavity configuration has been studied in a Kerr-lens mode locked (KLM) Ti-sapphire laser [30]. When the optical Kerr effect was considered as the nonlinear dynamical parameter, optical bistability and multiple-period bifurcation were numerically demonstrated. From the guidance, some peculiar phenomena were found by using an end-pumped Nd-YVO$_4$ laser under small-size pumping near g_1g_2 = 1/4: (1) Low lasing threshold and a power dip [31] occurred (see Fig. 1.3) nearly at the degeneracy of g_1g_2 = 1/4; (2) When an aperture was added in the cavity, a power peak instead of dip was at the degeneracy (see Fig. 1.4); (3) The beam waist shrinks abruptly near degeneracy; (4) The beam profile in the far field has many concentric rings (see Fig. 1.5). In particular, the beam could

exhibit three beam waists when it was propagated through a transform lens [32].

1.3   Aim of this research:

Since the gain saturation is the inherent nonlinear effect in lasers, the configuration-dependent dynamics near the low-order resonances may exhibit some important behaviors.   In this research we numerically investigate the nonlinear dynamics of a simple plano-concave end-pumped Nd-YVO$_4$ laser near the degenerate resonator configurations by using Collin's integral together with the rate equations. Because the excited transverse modes would be different by controlling the pump size or the gain volume of the active medium, our studies were divided into two parts: the pump size w_p is larger than and is less than the fundamental Gaussian beam waist w_c. We found that these two cases exhibit very different dynamical behaviors as we anticipated.

For the case of $w_p > w_c$, we found the propagation-dominant instabilities and chaos under high-Q cavity condition near $g_1g_2 = 1/4$ that had not numerically studied before.   We call it "propagation dominant" because the laser behaves as a conservative system governed by the beam propagation.   We also obtained a V-shaped configuration-dependent quasi-periodic threshold.   Although chaos were previously predicted impossible under nearly degenerate configurations, we have recognized that the laser is transformed into chaos as a result of the interplay of beam propagation and gain dynamics as the cavity is tuned close to degeneracy.

For the case of $w_p < w_c$, we found there are the stationary modes that show an additional beam waist besides the well-known waist on the flat mirror end near $g_1g_2 = 1/4$ and 3/4.   The numerical results show good agreement with the previous experimental observations that the specific modes were capable of exhibiting multiple beam waists when they were propagated through a transform lens.   The numerical

results give deep insight and lead to the other experimental observations near $g_1g_2 = 3/4$. In addition, by simultaneously considering the wavelike and the raylike character of the multibeam-waist mode, we found that it can be represented as a superposition of N consecutive round-trip electric fields of period-N solution in the degenerate empty cavity, where N = 2 for $g_1g_2 = 1/2$ and N = 3 for $g_1g_2 = 1/4, 3/4$.

Furthermore, we found that the laser instability occurs in a very narrow range of cavity tuning on each side of the point of degeneration, which shows periodic, period-doubling, and chaotic time evolutions as $w_p < w_c$. We determined both experimentally and numerically the unstable regions and clarify the origin of the instabilities. The temporal instabilities in the short-cavity side comes from the interaction among the transverse modes that constitute a supermode; while the long-cavity instabilities are spatiotemporal, which result from the nonlinear coupling between the supermode and the other Laguerre-Gaussian modes. These observed instabilities are new and, as far as we know, this is the first time to discuss the relationship between the instability and the thermal lens effect.

In Chapter 2, we focus on the dynamical behaviors induced by the wide pump ($w_p > w_c$) and compare our work with previous research. In Chapter 3, we study the multibeam-waist modes as $w_p < w_c$. In Chapter 4, we study the laser instabilities near the degeneracy when $w_p < w_c$. Finally, in Chapter 5 we state the conclusions and then give suggestions for future work.

References

[1]   E. Siegman, Lasers (Mill Vally, CA, 1986).

[2]   C.O. Weiss and R. Vilaseca, Dynamics of lasers (VCH, New York, 1991).

[3]   D.F. Nelson and W.S. Boyle, Appl. Opt. 1, 181 (1962).

[4]   C.L. Tang, H. Statz, G. deMars, J. Appl. Phys. 34, 2289 (1963).

[5]   A.Z. Grazyuk and A.N. Oraevskii, Quantum Electronics and Coherent Light, edited by P.A, Miles (Academic Press, New York, 1964).

[6]   J.A. Fleck and JR., R.E. Kidder," J. Appl. Phys. 35, 2825 (1964).

[7]   H. Haken, Phys. Lett. 53A, 77 (1975).

[8]   C.O. Weiss and J. Brock, Phys. Rev. Lett. 57, 2804 (1986).

[9]   L.W. Casperson, IEEE J. Quantum Electron. 14, 756 (1978).

[10] N.B. Abraham, L.A. Lugiato, P. Mandel, L.M. Narducci, and D.K. Bndy, J. Opt. Soc. Am. B 2, 35 (1985).

[11] L.W. Casperson, J. Opt. Soc. Am. B 2, 62 (1985); J. Opt. Soc. Am. B 2, 73 (1985).

[12] R.S. Gioggia and N. B. Abraham, Phys. Rev. Lett. 51, 650 (1983).

[13] H. Risken and K. Nummedal, J. Appl. Phys. 39, 4662 (1968).

[14] P. Graham and H. Haken, Z. Phys. 213, 420 (1968).

[15] E.M. Pessina, G. Bonfrate, F. Fontana, and L.A. Lugiato, Phys. Rev. A 56, 4086 (1997).

[16] K. Otsuka, Prog. in Quantum Electron. 23, 97 (1999).

[17] D. K. Bandy, A.N. Oraevskij, and J.R. Narducci, J. Opt. Soc. Am. B 5, 876 (1988), special issue on nonlinear dynamics of lasers; N.B. Abraham and W.J. Firth, J. Opt. Soc. Am. B 7, 951 (1990); L.A. Lugiato, Chaos, soliton, and fractals 4, 1251 (1994).

[18] L.A. Lugiato, C. Oldano, and L.M. Narducci, J. Opt. Soc. Am. B 5, 879 (1988).

[19] L.A. Lugiato, G.L. Oppo, M.A. Pernigo, J.R. Tredicce, and L.M. Narducci, Opt. Commun. 68, 63 (1988).

[20] L.A. Lugiato, F. Prati, L.M. Narducci, P. Ru, J.R. Tredicce, and D.K. Bandy," Phys. Rev. A 37, 3847 (1988).

[21] L.A. Lugiato, G.L. Oppo, J.R. Tredicce, L.M. Narducci, and M.A. Pernigo, J. Opt. Soc. Am. B 7, 1019 (1990).

[22] J.R. Tredicce, E.J. Quel, A.M. Ghazzawi, C. Green, M.A. Pernigo, L.M. Narducci, and L.A. Lugiato, Phys. Rev. Lett. 62, 1274 (1989);

[23] M. Brambilla, F. Battipede, L.A. Lugiato, V. Penna, F. Prati, C. Tamm, C.O. Weiss, Phys. Rev. A 43, 5090 (1991); M. Brambilla, M. Cattaneo, L.A. Lugiato, R. Pirovano, F. Prati, A.J. Kent, G.L. Oppo, A.B. Coates, C.O. Weiss, C. Green, E.J. D'Angelo, and J.R. Tredicce, Phys. Rev. A 49, 1427 (1994); A.B. Coates, C.O. Weiss, C. Green, E.J. D'Angelo, and J.R. Tredicce, M. Brambilla, M. Cattaneo, L.A. Lugiato, R. Pirovano, F. Prati, A.J. Kent, and G.L. Oppo, Phys. Rev. A 49, 1452 (1994).

[24] G. D'Alessandro and G.L. Oppo, Opt. Commun. 88, 130 (1992).

[25] W.Kaige, N.B. Abraham, and L.A. Lugiato, Phys. Rev. A 47, 1263 (1993); I. Boscolo, L.A. Lugiato, F. Prati, T. Benzoni, and A. Bramati, Opt. Commun. 115, 379 (1995).

[26] F. Hollinger and Chr. Jung, J. Opt. Soc. Am. B 2, 218 (1985); R. Hauck, F. Hollinger, and H. Weber, Opt. Commun. 47, 141 (1983); F. Hollinger, Chr. Jung, and H. Weber, Opt. Commun. 75, 84 (1990).

[27] A.G. Fox and T. Li, Bell Sys. Tech. J. 40, 453 (1961); IEEE J. Quantum Electron. 2, 774 (1966); IEEE J. Quantum Electron. 4, 460 (1968).

[28] M.D. Wei, W.F. Hsieh, and C.C. Sung, Opt. Commun. 146, 201 (1998).

[29] J.M. Greene, J. Math. Phys. 20, 1183 (1979); J.M. Greene, R.S. Mackay, F.

Vivaldi, and M.J. Feigenbaum, Physica D 3, 468 (1981).

[30] M.D. Wei and W.F. Hsieh, Opt. Commun. 168, 161 (1999); M.D. Wei, W.F. Hsieh, J. Opt. Soc. Am. B 17, 1335 (2000).

[31] H.H. Wu, C.C. Sheu, T.W. Chen, M.D. Wei, and W.F. Hsieh, Opt. Commun. 165, 225 (1999).

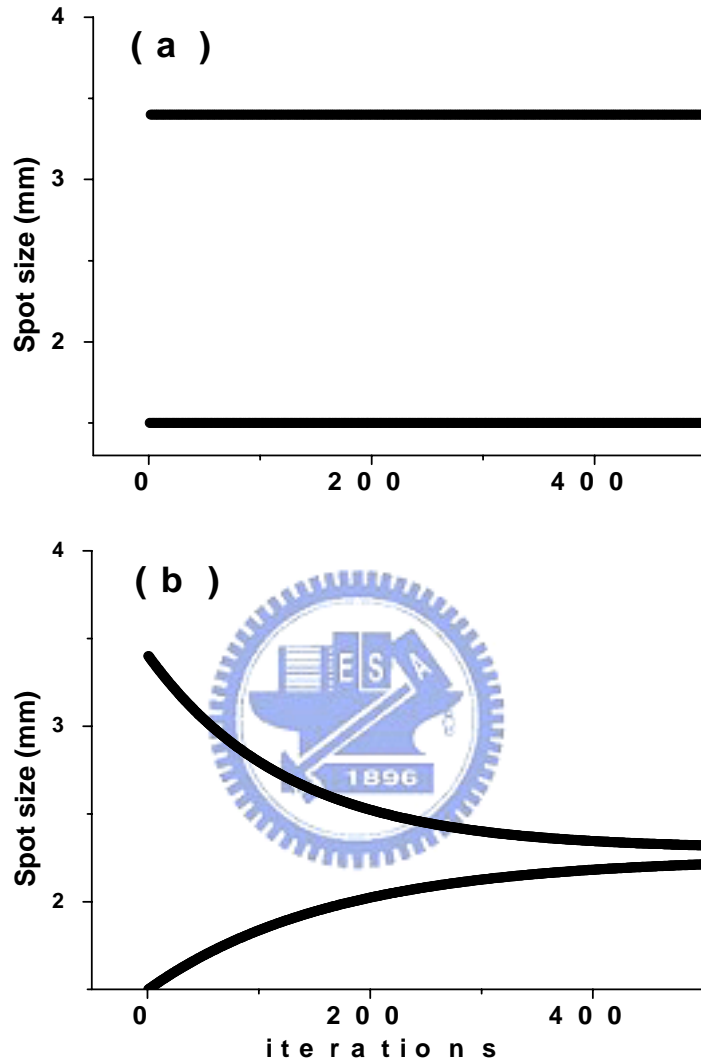[32] H.H. Wu and W.F. Hsieh, J. Opt. Soc. Am. B 18, 7 (2001).

Fig. 1.1.   Evolution of spot size as $g_1 g_2 = 1/2$ with initial values $(1/R_0, w_0) = (0, 1.5)$
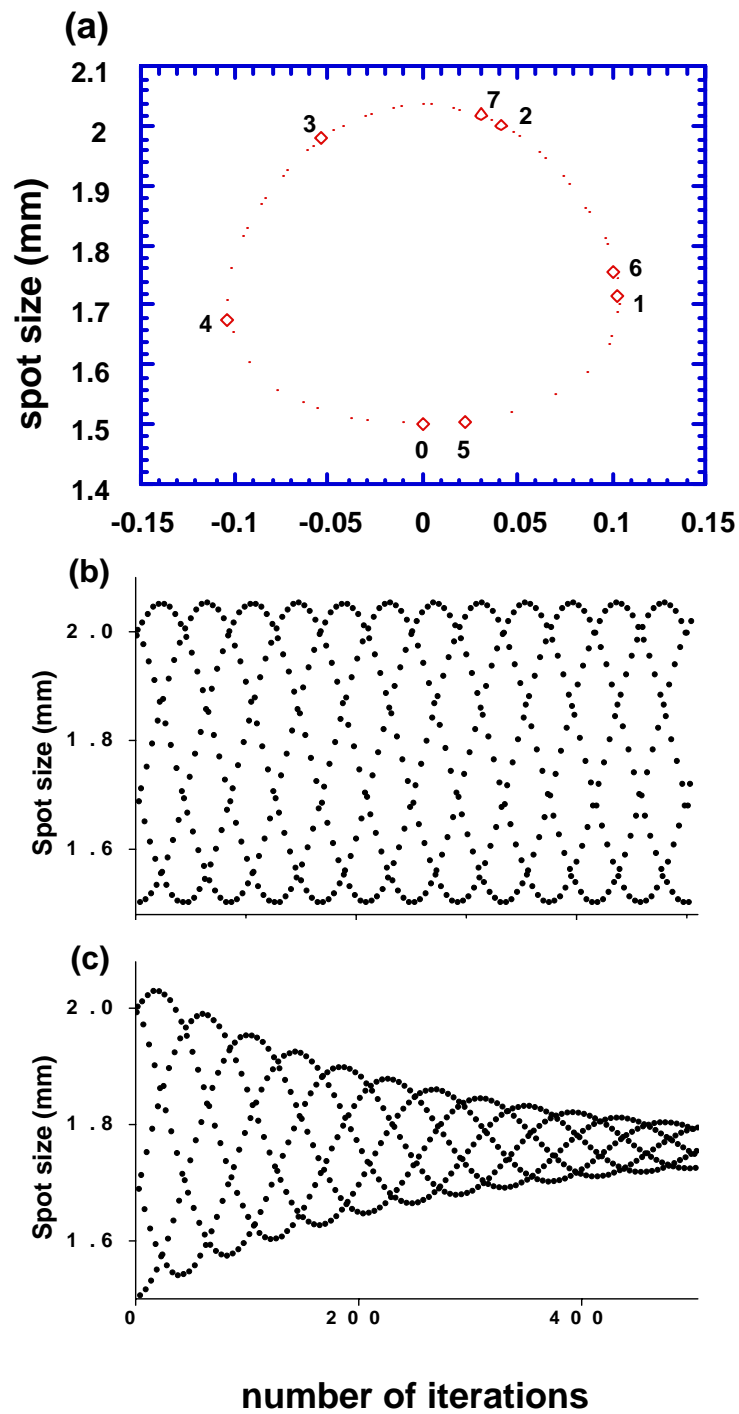
for conservative system (a) and for a Gaussian aperture inside (b).

Fig. 1.2. Evolution of iterative map for $g_1g_2 = 0.9$ with initial values $(1/R_0, w_0) = (0, 1.5)$ in phase space (a), the diamond marks with 0-7 represent the first 7 iterations; (b) the evolution of spot size for the same map as (a); (c) the evolution of spot size for a Gaussian aperture.
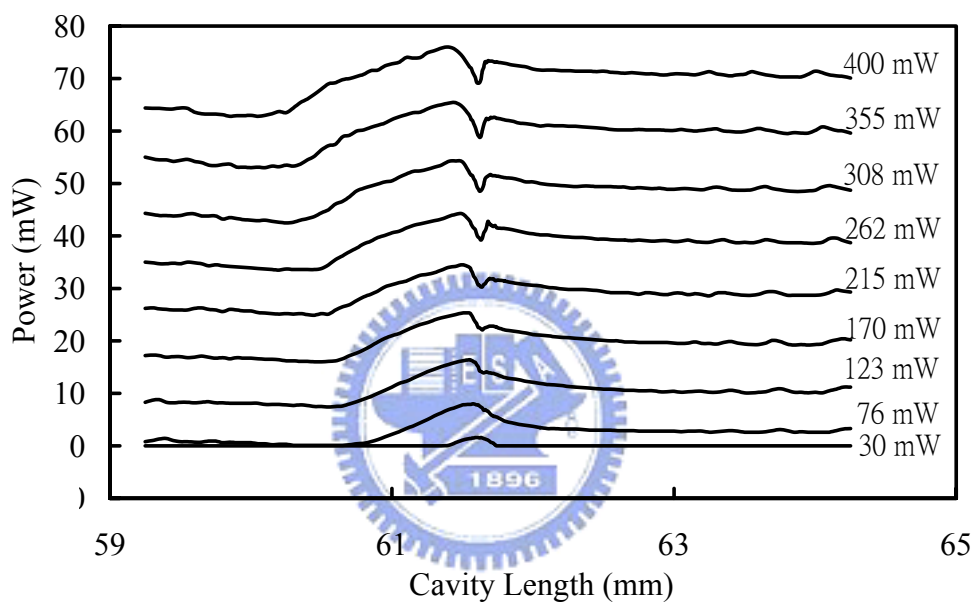
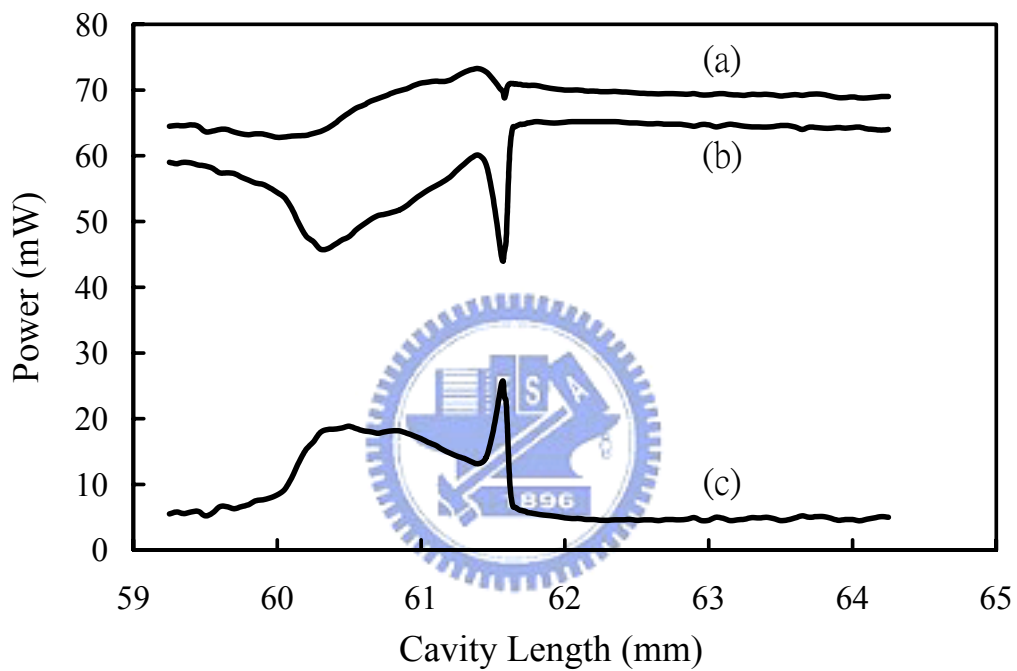Fig. 1.3. Total output power of the laser as a function of cavity length measured with different pumping power.

Fig. 1.4.   Average output power of a diode-pumped Nd:YVO$_4$ laser as a function of cavity length. Curve (a) measured without an aperture, curve (b) with an aperture, and curve (c) the difference between them.
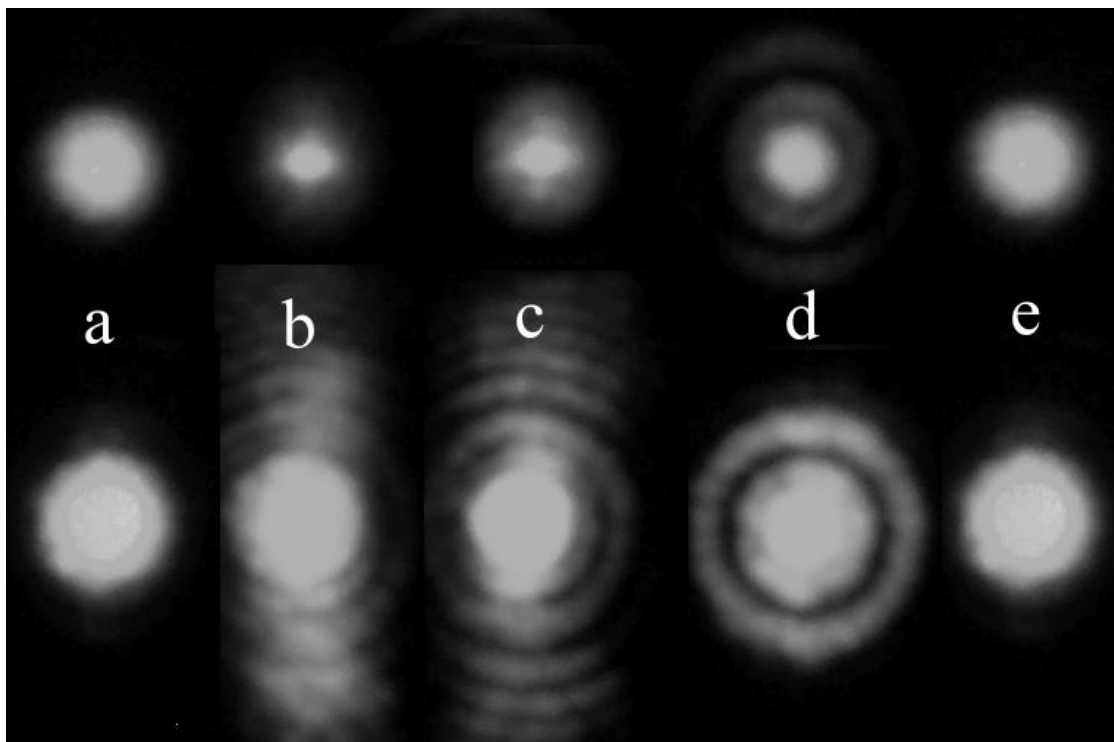
Fig. 1.5. Beam profile of the laser with different resonator configurations. Photographs shown in the upper and lower rows refer to near-field and far-field patterns, respectively. (a) and (e) away from, (b) and (c) near the degeneration point, and (d) in the power bump region.